

HYDROTHERMAL ALTERATION AND TOURMALINE-ALBITE EQUILIBRIA AT THE COXHEATH PORPHYRY Cu-Mo-Au DEPOSIT, NOVA SCOTIA*

GREGORY LYNCH¹ AND JORGE ORTEGA

*Geological Survey of Canada, Centre Géoscientifique de Québec,
2535 boulevard Laurier, C.P. 7500, Sainte-Foy, Québec G1V 4C7*

ABSTRACT

The Coxheath deposit is a zoned Cu-Mo-Au porphyry system related to Hadrynian calc-alkaline volcanic and plutonic rocks of the Avalon Zone in northeastern Nova Scotia. Alteration minerals are distributed over 30 km², and cross the contact of a composite porphyritic granitic pluton and overlying volcanic units. In the core of the pluton, a zone of potassic alteration comprises quartz-feldspar stockwork veinlets that contain varying proportions of chalcopyrite + bornite + molybdenite and accessory magnetite + hematite. Hydrothermal titanite, apatite, and actinolite also occur. Peripheral to the potassic zone, propylitic alteration assemblages contain chlorite + epidote + calcite + pyrite in veins or as patchy replacements. Farther outward, volcanic units have been affected by widespread and intense phyllic alteration and sericitization, and by the formation of quartz stockworks and up to 2-5% disseminated pyrite. The outermost zones were overprinted by argillic alteration, characterized by kaolinite, pyrophyllite, and local chalcedonic quartz. Tourmaline occurs in stockwork veinlets with albite, defining a restricted zone of sodic alteration that overlaps the central potassic zone and inner margin of the propylitic zone. Compositions of the tourmaline tend toward dravite, with significant dravite-povondraite solid solution marked by Fe-Al exchange in the octahedral site. A minor proportion of the uvite component and charge balance according to stoichiometry indicate $Fe^{2+}/(Fe^{2+} + Fe^{3+})$ values of 0.4 to 0.9. Fluid-mineral equilibria at the hematite-magnetite buffer suggest that tourmaline precipitation is strongly influenced by cooling, and by the activity of boric acid, B(OH)₃. Boric acid is the dominant aqueous species of boron in hydrothermal systems, and is stable across a wide range in pH encompassing alkaline to acidic mineralizing conditions. As a relatively non-volatile component, modeling suggests that boric acid becomes concentrated in the liquid fraction of boiling fluids, contributing to the precipitation of tourmaline within the residual hydrothermal component, and enhancing the zoning of hydrothermal minerals.

Keywords: boric acid, tourmaline, povondraite, Coxheath porphyry deposit, boiling, Avalon Zone, Nova Scotia.

SOMMAIRE

Le gisement de Coxheath est un exemple d'un gisement zoné de type "porphyre à Cu-Mo-Au" lié à un cortège de roches hadryniennes calco-alkalines volcaniques et plutoniques de la zone avalonienne, dans le nord-est de la Nouvelle-Ecosse. Les assemblages de minéraux d'altération sont distribués sur une superficie de 30 km², traversant le contact entre un pluton composite de granite porphyrique et un cortège d'unités volcaniques sus-jacents. Dans le centre du pluton, une zone à altération potassique comprend un réseau de veinules à quartz + feldspath contenant des proportions variables de chalcopyrite + bornite + molybdénite, ainsi que magnétite + hématite accessoires. La titanite, l'apatite et l'actinolite, toutes d'origine hydrothermale, sont aussi présentes. Disposés de façon périphérique autour de la zone potassique, les assemblages d'altération propylitique contiennent chlorite + épidote + calcite + pyrite en veines ou en remplacements sous forme de taches. Encore plus loin du centre, les unités volcaniques ont subi les effets d'une altération phyllique et d'une séricitisation répandues et intenses, et de la formation de stockworks à quartz avec jusqu'à 2-5% de pyrite disséminée. Les zones externes montrent les effets d'une altération argillique, qui a produit kaolinite, pyrophyllite et, ici et là, du quartz, variété chalcédoine. La tourmaline se présente en réseaux de veinules avec de l'albite, et définit ainsi une zone restreinte d'altération sodique qui chevauche la zone centrale à altération potassique et la bordure interne de la zone d'altération propylitique. Les compositions de tourmaline sont dravitiques, mais tendent au pôle povondraïte, signalant un remplacement de Al par Fe appréciable dans la position octaédrique. Une composante mineure d'uvite et un bilan balancé des charges pour des compositions stoechiométriques indiquent des valeurs du rapport $Fe^{2+}/(Fe^{2+} + Fe^{3+})$ entre 0.4 et 0.9. Les équilibres entre minéraux et phase fluide aux conditions imposées par le tampon hématite - magnétite font penser que la précipitation de la tourmaline serait fortement favorisée par un refroidissement, et par l'activité de l'acide borique, B(OH)₃. L'acide borique serait l'espèce dominante du bore en milieu aqueux dans un système hydrothermal, et stable sur un grand intervalle de pH, allant de conditions favorisant la minéralisation en milieux alcalins à acides. Comme il s'agit d'une espèce

* Geological Survey of Canada contribution number 43295.

¹ E-mail address: lynch@gsc.nrcan.gc.ca

relativement peu volatile, notre modèle fait penser que l'acide borique devient concentré dans la fraction liquide d'un système en ébullition, contribuant ainsi à la précipitation de la tourmaline à partir du système hydrothermal résiduel, et ajoutant au schéma de zonation des minéraux hydrothermaux.

(Traduit par la Rédaction)

Mots-clés: acide borique, tourmaline, dravite, povondraïte, gisement de type "porphyre" de Coxheath, ébullition, zone avalonienne, Nouvelle-Ecosse.

INTRODUCTION

The Coxheath deposit, on Cape Breton Island in northeastern Nova Scotia (Fig. 1), is a vein and stockwork Cu–Mo–Au system. Since its discovery in 1875, it has undergone various phases of exploration and development, including extensive drilling, shaft sinking, and cross-cut driving (Oldale 1967). It was initially developed as a high-grade, low-tonnage prospect (Beaton & Sugden 1930), but eventual recognition of the porphyry-stockwork style of mineralization changed exploration strategies to that of a low-grade, high-tonnage prospect (Oldale 1967). Reported grades include values of up to 2% Cu, 1% MoS₂, and 8.6 ppm Au across limited widths (Oldale 1967). However, to date, only the core potassic zone, tourmaline veining, and propylitic zone of alteration within the deposit have been described (Oldale 1967, Hollister *et al.* 1974, Clarke *et al.* 1989).

In this study, we establish and document at the Coxheath deposit all of the zones that characterize typical porphyry systems, including the potassic core, phyllic margin, and outer argillic and epithermal assemblages, as well as propylitic (calcic alteration) and albite–tourmaline (sodic alteration) facies. Identification of these new zones has resulted in significant expansion of the area affected by the mineralized hydrothermal system. Surface mapping was carried out at various scales, and included detailed descriptions of trenches, excavated sites, and drill core. Petrographic examination was supplemented by X-ray diffraction and electron-microprobe analysis. Our study has emphasized tourmaline because of its

recognized association with the higher-grade parts of the deposit, and because it has considerable potential as a petrogenetic indicator mineral (*e.g.*, Henry & Guidotti 1985, Povondra & Novak 1986, Clarke *et al.* 1989).

Tourmaline is an important vein and alteration mineral that occurs in a wide variety of hydrothermal deposits, including different types of granite-related porphyry systems (Sillitoe 1973, Lynch 1989, Koval *et al.* 1991, London & Manning 1995), mesothermal Au veins (King & Kerrich 1986, Robert & Brown 1986, King 1990), and massive sulfide ores (Slack 1982, Taylor & Slack 1984, Palmer & Slack 1989), among others (*e.g.*, Clarke *et al.* 1989, Slack 1996). Compositionally, hydrothermal tourmaline spans a wide range between the schorl and dravite end-members, and in some deposits has a substantial Fe³⁺-rich or uvite component (Slack 1996). In zoned porphyry-stockwork Sn ± W deposits, tourmaline may be concentrated in parts of the potassic core and phyllic margin (Forsythe & Higgins 1990), where selective tourmalinization of host-rock shales can be common (Hsu 1943, Ahlfeld 1945, Lynch 1989). Tourmaline also is an abundant matrix mineral in breccia pipes spatially associated with, or cross-cutting, porphyry Cu deposits in volcanic terranes (Sillitoe & Sawkins 1971, Sillitoe 1973, Warnars *et al.* 1985, Lubis *et al.* 1994). In some cases, tourmaline occurs in high-level epithermal systems (Shelnutt & Noble 1985, Foit *et al.* 1989, Meldrum *et al.* 1994, Fuchs & Maury 1995). Tourmaline occurrences appear to be volumetrically most abundant in regions underlain by thick accumulations of clastic marine sediments (Ethier & Campbell 1977), by virtue of the high boron content of the argillaceous components of such sediments (Goldschmidt & Peters 1932, Landergren 1945, Harder 1959), or in volcanic arcs where boron is recycled during volcanic activity into upper crustal reservoirs from subducted sediments and altered oceanic crust (*e.g.*, Palmer 1991a, Bebout *et al.* 1993, Ishikawa & Nakamura 1994, Leeman *et al.* 1994, You *et al.* 1995).

Although field relations and experimental data demonstrate that tourmaline has a wide field of stability, parameters that control the mobilization and transport of boron, and the precipitation of tourmaline, are not well understood. Low-temperature authigenic tourmaline from limestone and sandstone has been reported by many investigators (*e.g.*, Krynine 1946, Robbins & Yoder 1962, Henry & Dutrow 1992); tourmaline is a well-known constituent of medium- to high-grade pelitic schists (Henry & Guidotti 1985), and is common as a primary igneous phase in pegmatites (*e.g.*, Joliff *et al.*

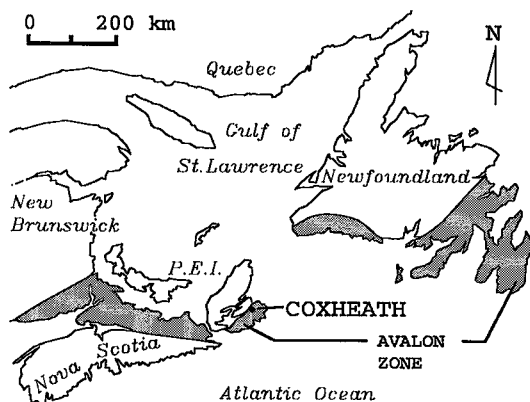


FIG. 1. Map showing location of the Coxheath porphyry Cu–Mo–Au deposit within the Avalon Zone of the Canadian Appalachians.

1986) and as a late-magmatic to hydrothermal phase within orbicules in granites (Sinclair & Richardson 1992). At its upper stability limit near 900°C, hydrothermal tourmaline breaks down to form spinel + cordierite (Fuh 1965), or kornepurine + sapphirine (Robbins & Yoder 1962). Other experimental results (Vorbach 1989) suggest a more restricted field of stability for hydrothermal tourmaline, approximately 250°–750°C. Pressure apparently does not exercise a strong control on the stability of tourmaline (Fuh 1965), but solutions of intermediate pH with low to high solute concentrations favor its precipitation (Smith 1949, Morgan & London 1989). And fluid inclusions in tourmaline from

mineralized breccias at El Teniente in Chile record hypersaline fluids (34–44 wt.% NaCl equivalent), under boiling conditions at 300°–400°C (Skewes 1992).

GEOLOGICAL SETTING

The Avalon Zone of the Canadian Appalachians (Fig. 1) is characterized by a vast Late Proterozoic volcano-plutonic arc, constructed on a Gondwana basement, with correlative units extending to other portions of the North Atlantic, Africa, and South America (Williams 1984). On Cape Breton Island, the Avalon Zone contains five volcanic belts (Barr *et al.* 1988), ranging in age

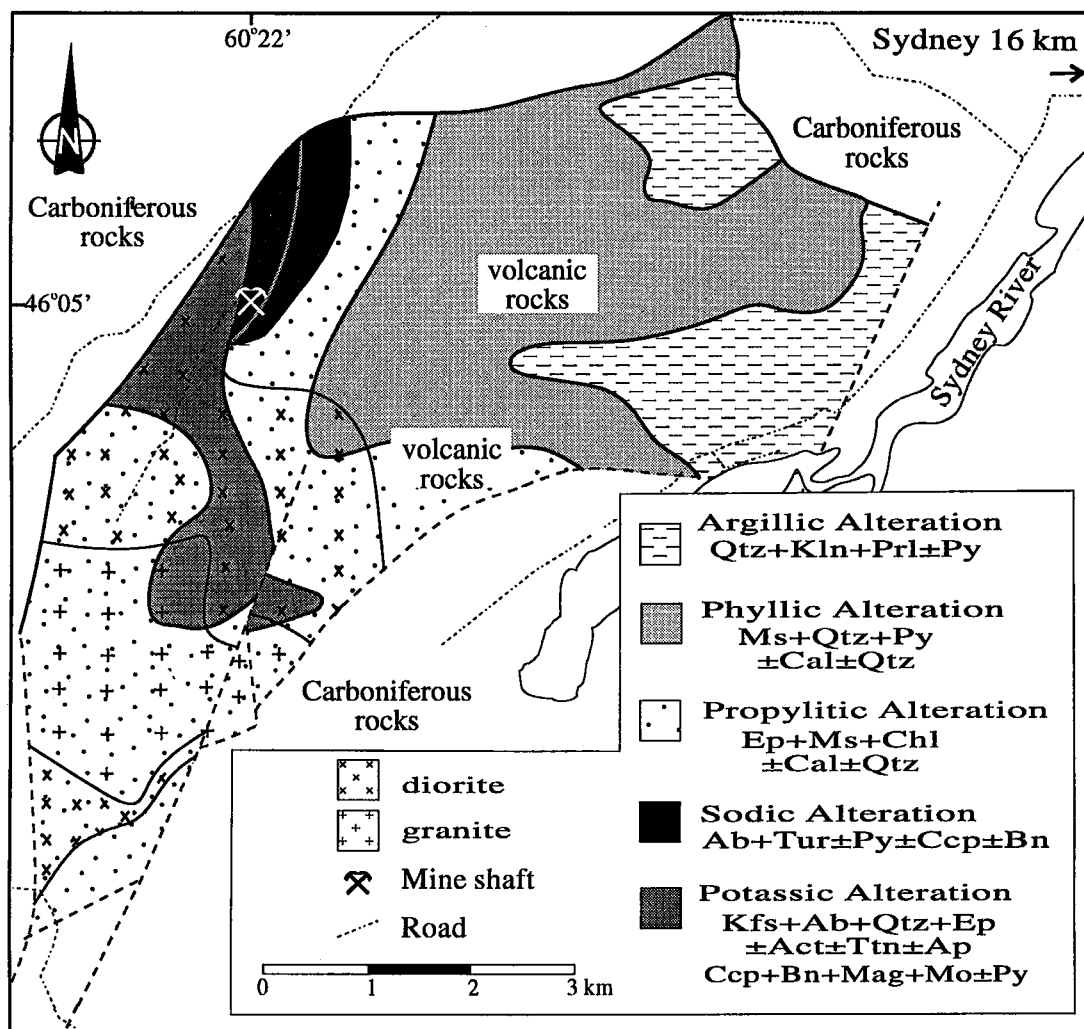


FIG. 2. Geology and alteration map of the Coxheath deposit. Mineral abbreviations are as follows: quartz (Qtz), calcite (Cal), epidote (Ep), chlorite (Chl), actinolite (Act), apatite (Ap), titanite (Ttn), tourmaline (Tur), albite (Ab), K-feldspar (Kfs), kaolinite (Kln), pyrophyllite (Prl), sericite (Ser), muscovite (Ms), pyrite (Py), chalcocopyrite (Ccp), bornite (Bn), molybdenite (Mo), magnetite (Mag).

from 575 to 680 Ma (Bevier *et al.* 1993). However, unconformably overlying Cambrian–Ordovician, as well as extensive Devonian–Carboniferous sedimentary rocks, cover much of the region. Metamorphism typically is only weakly developed within the Proterozoic units, being of subgreenschist to lower-greenschist grade. Rocks of the Coxheath belt in the vicinity of the Coxheath Cu–Mo–Au deposit consist of flows and pyroclastic deposits ranging in composition from basalt, andesite, and dacite, to rhyolite. Geochemical studies have identified a calc-alkaline trend (Thicke 1987, Dostal & McCutcheon 1990, Barr 1993), with trace-element patterns indicating a continental-margin arc setting (Dostal & McCutcheon 1990). The volcanic rocks are cut by a large composite pluton comprising a core of granite to granodiorite and a broad margin of diorite to monzonite containing an abundance of volcanic xenoliths. The diorite, typically fine- to medium-grained and equigranular, grades inward to porphyritic monzonite that displays scattered, very coarse phenocrysts of plagioclase. The granitic core is medium-grained and equigranular, and locally contains xenoliths of diorite, indicating a cross-cutting relationship with the border phase. However, compositional variations within the pluton are thought to have resulted from *in situ* differentiation of the crystallizing magma (Chatterjee & Oldale 1980).

Rhyolite within the Coxheath belt has been dated at 613 ± 15 Ma by the U–Pb zircon method (Bevier *et al.* 1993). The composite pluton described above has

yielded $^{40}\text{Ar}/^{39}\text{Ar}$ ages of 621.9 ± 4.2 Ma and 620.6 ± 4.7 Ma, obtained from hornblende interpreted to be of igneous origin (Keppie *et al.* 1990). Within the error limits of the dating methods, the pluton and volcanic rocks thus may be coeval. Bedding in the volcanic succession typically is poorly defined. Carboniferous normal faults bound much of the Proterozoic units, with the most pronounced set striking north–northeast and having a subvertical dip.

HYDROTHERMAL ALTERATION AND MINERAL ZONING

Hydrothermal alteration and stockwork veining of varying intensity have been documented across an area of approximately 30 km², measuring 7 by 4 km. Five principal zones (Fig. 2) comprise the alteration types typical of porphyry Cu–Mo–Au and epithermal systems (*e.g.*, Lowell & Guilbert 1970, Sillitoe 1993). From the plutonic core to the outer overlying volcanic edifice, these consist of potassic, tourmaline, propylitic, phyllic, and argillic zones. Mineral parageneses of the principal vein-types and alteration facies are summarized in Figure 3, based on cross-cutting relations established by field and petrographic observations.

Potassic zone

Two sets of stockwork veinlets occur in each of the monzonite and diorite border phases of the Coxheath pluton. Within the central part of the monzonite body,

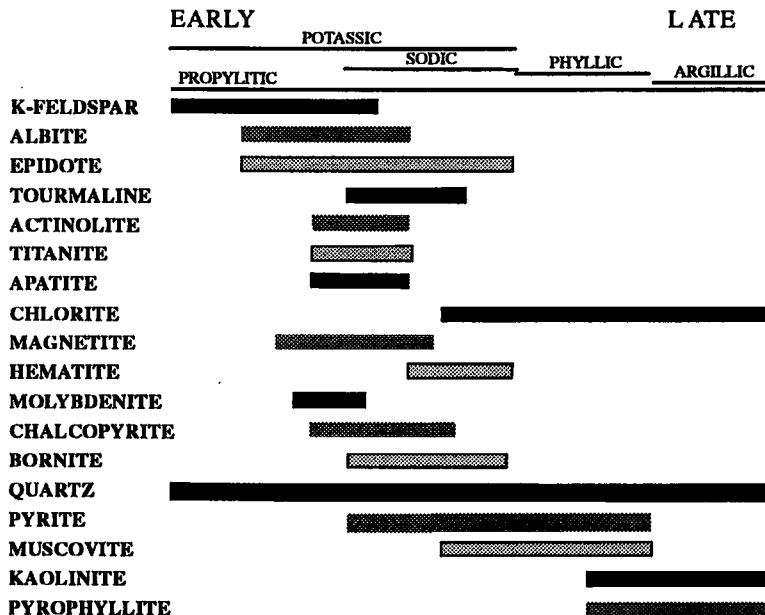


FIG. 3. Paragenesis diagram of principal vein and alteration minerals. Designation of early and late is an approximation based on cross-cutting relations and overlapping mineral assemblages.

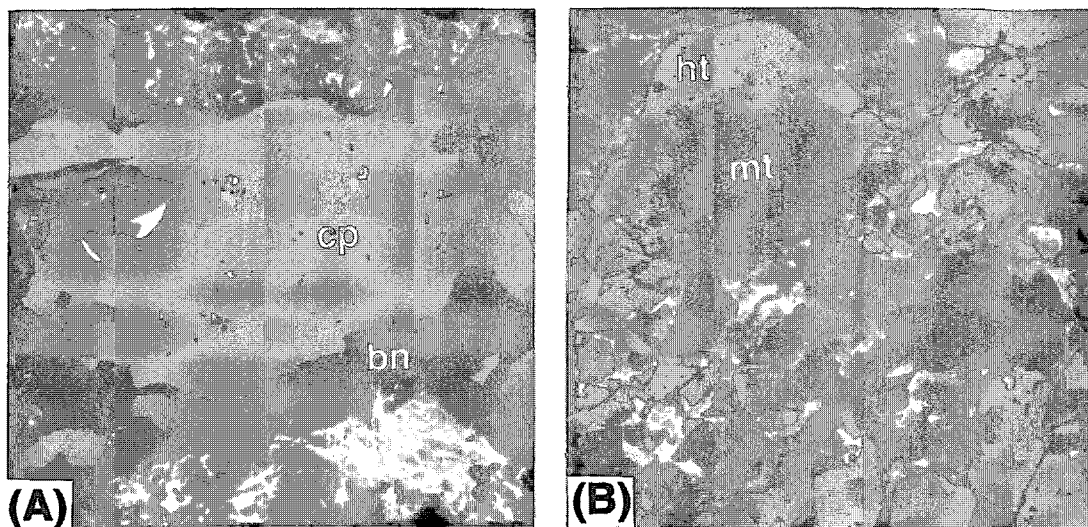


FIG. 4. Photomicrographs of (A) vein chalcopyrite (light grey, cp) rimmed by a layer of bornite (dark grey, bn); (B) hematite rim (light grey, ht) on magnetite (dark grey, mt). Both samples are from the potassic zone. Field of view is 1 mm along base for (A) and 0.7 mm for (B).

quartz veinlets have developed a strong alteration-halo dominated by K-feldspar accompanied by varying amounts of albite, epidote, apatite, as well as veinlet or disseminated chalcopyrite, and pyrite. Veins in the second set contain quartz with actinolite, surrounded by a halo of K-feldspar, titanite, and apatite, with disseminated or veinlet chalcopyrite, bornite, pyrite, and magnetite. Bornite typically occurs as a rim on chalcopyrite (Fig. 4A), associated with varying proportions of pyrite or magnetite. Outward, to the diorite margin, the potassic alteration facies lacks pyrite, but contains molybdenite and magnetite. Within the diorite, quartz veinlets display a halo of K-feldspar with variable amounts of albite, epidote, chlorite, titanite, and apatite, as well as vein or disseminated chalcopyrite, bornite, molybdenite, and magnetite. Magnetite commonly has either a hematite rim (Fig. 4B), or hematite developed along cleavage and fracture planes. Coarse specular hematite also is observed, and occurs as radial aggregates disseminated in the altered rock. Bornite forms a rim on chalcopyrite, or is intergrown with chalcopyrite and molybdenite. A late set of quartz–molybdenite veins associated with a K-feldspar halo cuts earlier stockworks of potassic alteration in the diorite, and comprises thicker veins that may be up to 20 cm thick. Late-stage, fine-grained muscovite alters hydrothermal feldspar in the potassic zone, and quartz–muscovite veins locally cut K-feldspar veinlets.

Although secondary K-feldspar is the characteristic mineral of the potassic alteration facies, secondary albite defines a clear sodic component to the alteration assemblage; actinolite, titanite, apatite, and epidote compose a distinctive calcic component. The sodic and calcic

components are interpreted to reflect alteration of igneous plagioclase in the plutonic rocks, whereas titanium for the hydrothermal titanite was likely derived from the breakdown of hornblende during hydrothermal alteration. On the basis of the abundance of K-feldspar in this hydrothermal zone, we infer that potassium was introduced during alteration. Also, molybdenite is concentrated outward, away from the monzonite and toward the diorite border phase.

Tourmaline–albite zone

The tourmaline zone is defined by the presence of tourmaline, and is limited to diorite near its northeastern contact with the volcanic units. Here, quartz–tourmaline veins form complex stockworks that overprint rocks previously affected by potassic alteration. In some outcrops, steeply dipping veins of tourmaline strike predominantly north–northeast. Where dense clusters of stockwork veinlets occur, the host may be completely black owing to replacement by tourmaline. Tourmaline selvages along the vein margins typically are 1–2 cm wide, and progress outward to solid pink albite selvages, also 1–2 cm wide, in a small-scale zoned configuration. Quartz, tourmaline, and albite occur with accessory muscovite, chlorite, and epidote. The veins are strongly zoned, with alternating encrustations of layers composed of either quartz + tourmaline, or pyrite with accompanying chalcopyrite and bornite. A sharp segregation of the layered assemblages is common. Single layers within a vein are generally less than 0.5 cm thick; however, a vein may be as wide as 3–5 cm. Tourmaline occurs as subhedral to euhedral

randomly oriented crystals, with a dark brown coloration and no apparent internal zoning.

Propylitic, phyllic, and argillic zones

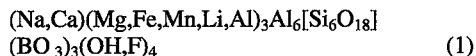
Disseminated epidote or veinlet calcite, epidote, chlorite, and accessory pyrite characterize the propylitic assemblage. Propylitic alteration occurred in the volcanic units adjacent to the margins of the pluton, as well as within western outcrops of the granite; it also completely overprinted the potassic and tourmaline-bearing alteration zones, as distinct cross-cutting sets of late propylitic veins. The intensity of the propylitic alteration is variable, and in portions of the zone, it is quite weak. In contrast, phyllic alteration is intense through most of the phyllic zone, where pervasive sericitization, silicification, and pyritization (5–10% pyrite) replaced much of the rock and destroyed primary textures. The phyllic zone covers a wide area within the volcanic rocks away from the pluton and central zones of alteration (Fig. 2). Very thin veinlets of quartz form subtle stockworks. In outcrop, the phyllic alteration is striking owing to a white coloration and abundance of rust staining.

The argillic zone occurs at the eastern end of the hydrothermal system, adjacent to the phyllic zone, and is unconformably covered by Carboniferous clastic sedimentary rocks to the east. This zone is characterized by fine-grained clay minerals and an intense silicification of the host rock. Both kaolinite and pyrophyllite were identified by X-ray diffraction. The degree of silicification is greater in this zone relative to the other alteration facies. Large exposures of rock occur that are almost completely converted to very fine-grained

quartz, with minor associated clay and pyrite. Minute veinlets of quartz are found in much of the rock, and locally, veins up to 20 cm wide contain very fine-grained quartz or chalcedonic quartz. The host rock in this zone is predominantly rhyolite, which can be identified by the presence of squarish paramorphs after β -quartz.

TOURMALINE CHEMISTRY

Tourmaline is a chemically complex mineral with a large number of possible substitutions; it has the following generalized formula:



A site-reference scheme may be represented by $(R1)(R2)_3(R3)_6(\text{BO}_3)_3\text{Si}_6\text{O}_{18}(\text{OH,F})_4$, with R1 representing Na, Ca, K, or vacant; R2 representing Fe^{2+} , Mg, Mn^{2+} , and Fe^{3+} , Cr^{3+} , V^{3+} , Ti^{4+} , or Al (where R1 is vacant), or Li (where coupled with Al substitution), and R3 representing Al, Fe^{3+} , Cr^{3+} , V^{3+} , and Fe^{2+} or Mg (where coupled by Ca substitution in R1), or 1.33 Ti^{4+} (Burt 1989, London & Manning 1995). Also, it has been shown that Al may substitute for Si in the tetrahedral site (Hawthorne 1996). The numerous possible substitutions within tourmaline, as well as its wide field of stability, render it a useful petrogenetic indicator mineral for discriminating mineralizing regimes (Henry & Guidotti 1985, Povondra & Novák 1986, Slack 1996). As many as eleven end-members have been defined.

Results of thirty-one analyses of tourmaline from the Coxheath deposit are presented in Table 1. The chemical analyses were obtained at the Geological Survey of Canada in Ottawa, using a Cameca SX-50 electron microprobe. Quantitative wavelength-dispersion analyses (WDA) were done at 15 kV accelerating potential, and 10–20 s counting time. Standards used include NaCl (Na), KBr (K), wollastonite (Ca), corundum (Al), quartz (Si), MgO (Mg), and pure metal standards for each of Mn, Ti, Cr, V, and Fe. However, Mn, Cr, and

TABLE 1. ELECTRON-MICROPROBE DATA ON TOURMALINE FROM COXHEATH

	T-1	T-2	T-3	T-4	T-6	T-7	T-8	T-9	T-10	T-11	T-12
SiO ₂	33.68	35.45	34.77	34.28	34.04	35.17	34.84	34.33	34.30	33.40	33.65
Al ₂ O ₃	22.62	27.80	27.10	24.80	22.33	25.70	26.98	28.04	25.44	23.10	24.57
MgO	7.28	7.66	8.22	8.48	7.34	7.47	7.40	7.24	7.17	7.02	6.80
TiO ₂	0.79	0.23	0.36	0.71	0.42	0.22	0.29	0.59	0.76	0.71	0.78
FeO	17.34	10.22	10.89	12.54	17.57	13.75	12.04	14.61	14.55	14.11	16.55
Na ₂ O	1.80	2.25	2.12	1.80	1.73	2.19	2.15	1.91	2.05	1.78	1.89
CaO	1.92	0.78	1.25	1.88	2.00	1.14	1.31	1.71	1.49	1.98	1.65
K ₂ O	0.01	0.06	0.03	0.04	0.02	0.03	0	0.01	0.03	0.08	0
TOTAL	85.44	84.45	84.74	84.53	85.45	85.67	85.01	85.64	85.79	85.18	85.89

FORMULA (BASIS 24.5 ATOMS OF OXYGEN)

Si	5.993	6.056	5.967	5.983	6.058	6.064	5.994	6.003	5.954	5.998	5.910
Al	4.744	5.598	5.481	5.101	4.685	5.222	5.472	5.131	5.203	4.678	5.085
Mg	1.931	1.950	2.103	2.207	1.948	1.919	1.897	1.878	1.856	1.879	1.782
Ti	0.106	0.033	0.047	0.099	0.057	0.029	0.038	0.077	0.099	0.096	0.104
Fe	2.981	1.460	1.563	1.830	2.616	1.983	1.737	2.124	2.112	2.721	2.431
Na	0.620	0.746	0.706	0.609	0.597	0.733	0.716	0.642	0.689	0.618	0.645
Ca	0.366	0.144	0.231	0.351	0.381	0.210	0.242	0.320	0.278	0.380	0.310
K	0.002	0.013	0.007	0.009	0.005	0.008	0	0.002	0.006	0.019	0.001
TOTAL	16.341	15.993	16.103	16.182	16.344	16.167	16.091	16.176	16.195	16.387	16.267

	T-13	T-14	T-15	T-16	T-17	T-18	T-19	T-20	T-21	T-22	T-23
SiO ₂	34.73	34.60	35.39	34.22	34.89	34.29	34.47	34.42	34.54	34.11	35.12
Al ₂ O ₃	27.24	26.30	27.93	23.28	25.96	26.71	25.54	25.50	26.05	25.15	27.88
MgO	7.13	7.90	7.60	7.360	7.47	7.20	7.50	7.18	6.67	7.42	7.52
TiO ₂	0.55	0.27	0.34	0.62	0.41	0.52	0.33	0.53	0.16	0.63	0.27
FeO	11.28	12.46	10.71	16.73	13.26	12.65	12.46	13.65	13.78	14.08	10.77
Na ₂ O	2.38	2.23	2.27	4.89	2.75	5.41	5.31	5.94	5.34	5.180	5.613
CaO	0.75	1.18	0.92	1.75	1.44	1.43	1.40	1.54	1.45	1.58	0.98
K ₂ O	0.04	0.02	0.12	0.03	0.03	0.04	0.03	0.04	0.03	0.05	0.03
TOTAL	84.1	84.96	85.28	85.88	85.59	84.94	84.29	84.93	84.81	85.12	84.83

FORMULA (BASIS 24.5 ATOMS OF OXYGEN)

Si	6.008	5.991	6.013	6.022	6.014	5.937	6.010	6.001	6.024	5.960	6.000
Al	5.554	5.438	5.493	4.899	5.275	5.451	5.331	5.241	5.354	5.180	5.613
Mg	1.942	2.036	1.924	1.932	1.820	1.859	1.850	1.866	1.734	1.934	1.915
Ti	0.019	0.035	0.044	0.082	0.054	0.068	0.044	0.069	0.022	0.083	0.035
Fe	1.632	1.802	1.522	2.463	1.911	1.832	1.817	1.991	2.010	2.028	1.539
Na	0.798	0.747	0.748	0.644	0.711	0.705	0.730	0.699	0.721	0.712	0.749
Ca	0.139	0.219	0.167	0.350	0.266	0.266	0.288	0.271	0.295	0.180	0.285
K	0.009	0.006	0.026	0.008	0.008	0.009	0.007	0.009	0.007	0.011	0.006
TOTAL	16.100	16.161	16.033	16.308	16.155	16.126	16.149	16.163	16.141	16.230	16.036

TABLE 1. CONTINUED

	T-24	T-25	T-26	T-27	T-28	T-32	T-33	T-34	T-35	T-36
SiO ₂	34.69	33.86	35.44	35.25	34.3	35.14	35.26	35.95	35.42	35.90
Al ₂ O ₃	23.42	22.52	27.46	26.45	26.19	28.07	29.33	30.30	26.77	29.67
MgO	7.70	6.86	7.80	7.54	7.34	7.74	7.12	7.72	8.79	7.92
TiO ₂	0.38	0.70	0.28	0.34	0.45	0.12	0	0.03	0.12	0.34
FeO	16.00	17.45	11.89	12.44	13.73	11.32	10.76	8.33	9.89	9.33
Na ₂ O	2.62	1.81	2.19	2.20	1.93	2.06	1.88	2.10	1.94	2.38
CaO	0.65	2.07	1.11	1.28	1.65	1.42	1.19	0.53	1.57	1.61
K ₂ O	0.04	0.03	0.02	0.02	0.03	0.01	0.06	0.02	0	0.04
TOTAL	85.40	85.30	86.19	85.52	85.62	85.88	85.62	84.98	85.40	86.59

FORMULA (BASIS 24.5 ATOMS OF OXYGEN)

Si	6.098	6.038	5.999	6.042	5.933	5.953	5.953	6.008	5.999	5.952
Al	4.853	4.734	5.478	5.344	5.338	5.604	5.838	5.968	5.344	5.978
Mg	2.017	1.823	1.968	1.927	1.893	1.956	1.791	1.924	2.221	1.958
Ti	0.051	0.094	0.036	0.045	0.058	0.016	0	0.003	0.131	0.042
Fe	2.352	2.603	1.683	1.784	1.986	1.605	1.519	1.164	1.401	1.294
Na	0.893	0.627	0.718	0.731	0.648	0.678	0.615	0.682	0.639	0.765
Ca	0.104	0.395	0.202	0.233	0.306	0.238	0.215	0.096	0.285	0.180
K	0.010	0.006	0.005	0.005	0.008	0.003	0.013	0.005	0	0.008
TOTAL	16.576	16.319	16.088	16.110	16.169	16.071	15.943	15.848	16.019	15.994

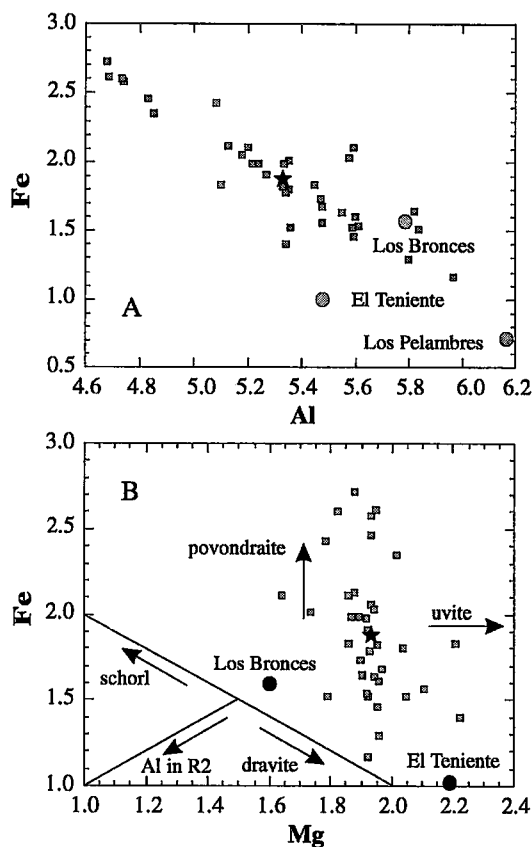


FIG. 5. Plots of tourmaline composition. (A) Fe versus Al, and (B) Fe versus Mg, in atoms per formula unit (*apfu*) for tourmaline from the Coxheath deposit. For comparison with other porphyry Cu deposits, average values for tourmaline from the Los Bronces, El Teniente, and Los Pelambres deposits in Chile also are shown (Skewes 1992). Arrows in (B) emphasize trends toward end-member compositions, as well as fields for Al-rich (Al in R2) and Al-poor (upper right-hand field) tourmaline. Star symbol is average value for Coxheath samples.

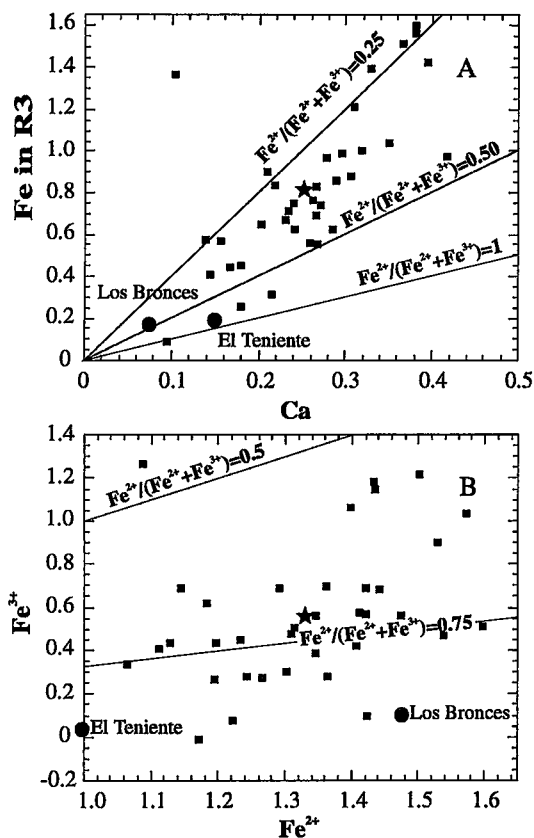


FIG. 6. Plots of tourmaline composition (A) Total Fe in R3 versus Ca, and (B) calculated Fe^{3+} versus Fe^{2+} , in atoms per formula unit for tourmaline from the Coxheath deposit. The amount of ferric iron in the R3 site was calculated as the total amount of Fe in R3 in excess of the number of Ca atoms in R1 [$Fe^{3+} = Fe - (3 - Mg) - Ca$]. Star symbol is the average value for Coxheath samples. Note that the ratio of ferrous to ferric iron in (A) refers to proportions within the R3 site only, whereas the ratios in (B) are for total iron including both R2 and R3 sites.

V are below detection limits or present in trace amounts and are not included in Table 1.

Oxide totals for most analyses are near 85%. The SiO_2 contents are quite uniform at 34–35 wt.%, approximating 6 atoms per formula unit (*apfu*) Si. Fe and Al show the greatest amount of variability (Fig. 5A); Mg is remarkably uniform at close to 2 *apfu* (Fig. 5B). Fe varies by 1.5 *apfu*, from 1.2 to 2.7, whereas Al varies by 1.3 *apfu*, from 4.7 to 6.0 (Fig. 5A, Table 1). The Fe versus Al plot in Figure 5A shows a linear correlation defining a slope of approximately minus one, demonstrating that Fe substitutes directly for Al in the R3 site, since Al is below 6 *apfu*. Consequently, with Mg filling two thirds of the R2 site, Fe occupies a portion of both R2 and R3, requiring the likely presence of both ferrous

and ferric iron. The amount of Fe^{3+} in the R3 site may be approximated by the total amount of Fe in R3 in excess of the number of Ca atoms in R1 (*i.e.*, $Fe^{3+} = Fe - (3 - Mg) - Ca$; Fig. 6A), required for charge balance according to the following stoichiometry:



The $Fe^{2+}/(Fe^{2+} + Fe^{3+})$ value calculated in this manner ranges from 0.4 to 0.9, with an average value of 0.7 (Fig. 6B). Tourmaline at Coxheath shows only a limited uvite component, with Ca at 0.4 *apfu* or less, which allows for up to 1 atom of Fe^{3+} to reside in R3. The presence of ferric iron within Al-depleted R3 and

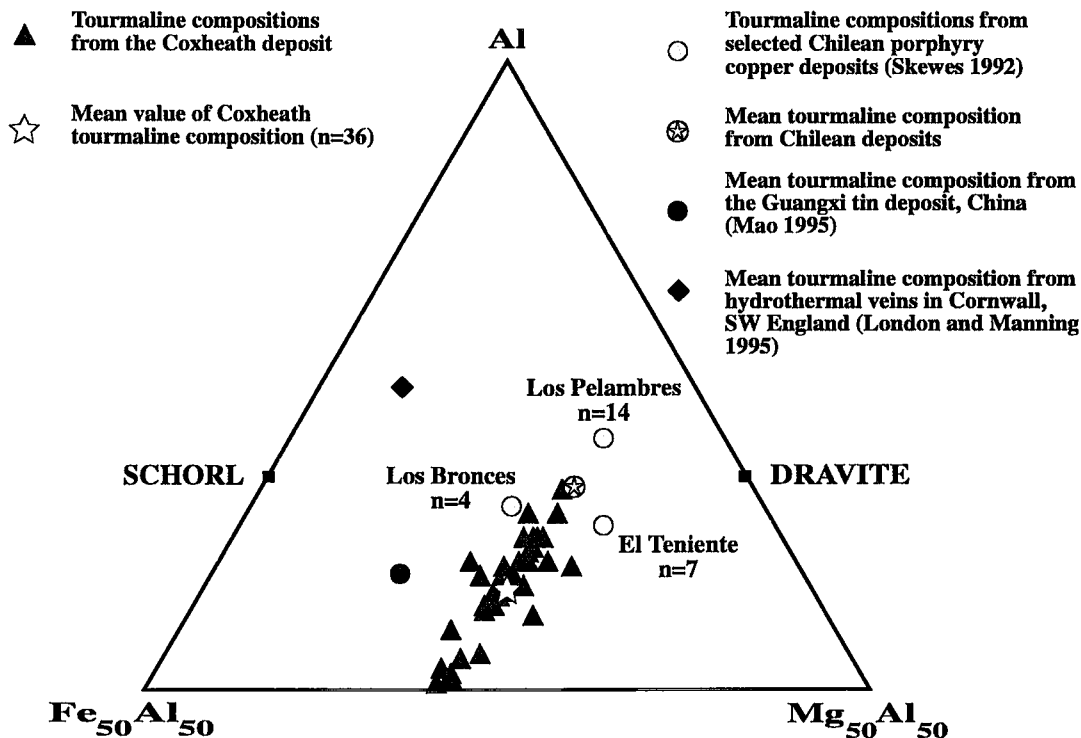


FIG. 7. Plot of tourmaline compositions on an $\text{Fe}_{\text{total}}\text{-Al-Mg}$ triangular diagram. The samples from Coxheath define a linear trend characterized by Fe-Al exchange in the field of Fe^{3+} -bearing tourmalines. Average values for samples from three other porphyry-Cu deposits fall close to this trend, whereas tourmaline from granite-related Sn deposits (diamond symbol) are typically Al-enriched and Mg-poor, tending more toward the schorl end-member.

the Mg dominance of R2 characterize this tourmaline as dravite with a povondraite component (*cf.* Grice *et al.* 1989). The average composition for Coxheath tourmaline is represented by the following formula:

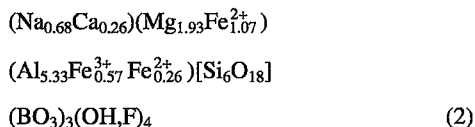


Figure 7 is an Al-Fe-Mg plot of tourmaline from Coxheath and other porphyry-stockwork systems. This plot displays the Al-Fe exchange, at relatively constant Mg, in the Coxheath tourmaline, as well as its distribution within the domain of ferric tourmaline. Tourmaline compositions from three Chilean porphyry-Cu deposits are plotted for comparison, and are close to the trend defined by the Coxheath tourmaline, although one has distinctly higher Al/Fe. Tourmaline from a number of other mineral deposits, mostly Sn \pm W stockwork systems, are characterized by a stronger tendency toward the schorl end-member (Fig. 7). These other tourmaline samples are for the most part distinguished by high Al

contents, with Al typically exceeding 6 *apfu*, filling R3 and part of the R2 sites.

ACTIVITY DIAGRAMS

Activity diagrams are commonly used when portraying equilibrium assemblages of alteration minerals and mineral reactions in porphyry systems. Mineralogical changes that occur across alteration zones have been extensively studied by a number of investigators, with emphasis placed on silicates, phyllosilicates, clay minerals, sulfides, and oxides. Although tourmaline is locally an important vein and alteration phase in porphyry systems, tourmaline-producing reactions have not been investigated or illustrated with activity diagrams. Aside from the inherent chemical complexity of tourmaline, one of the problems encountered is that it most often is the only boron-bearing phase present, in which case reactions that attempt to explain tourmaline precipitation must be balanced using aqueous boron species. On the one hand, boron in granitic magmas partially disrupts the aluminosilicate network, has a low solubility, and is largely expelled from magma as an incompatible

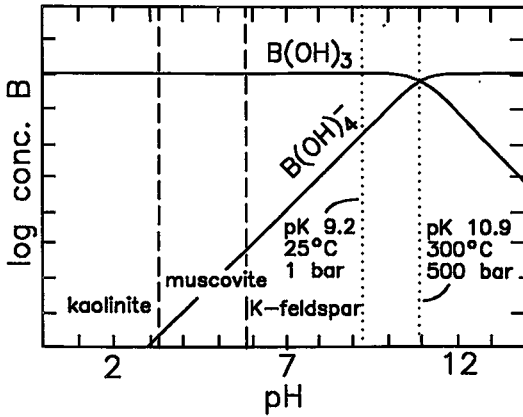


FIG. 8. Calculated concentration - pH diagram for boron under hydrothermal conditions demonstrates that boric acid $[B(OH)_3]$ is the dominant species at pH levels (e.g., $2 \leq \text{pH} \leq 7$) that encompass principal zones of alteration within porphyry systems. Equations for temperature- and pressure-dependent acidity constants for $B(OH)_3$ and $B(OH)_4^-$ speciation are from Gieskes (1974). An activity of 0.05 is used for K^+ in estimating the stability limits of silicates in terms of pH.

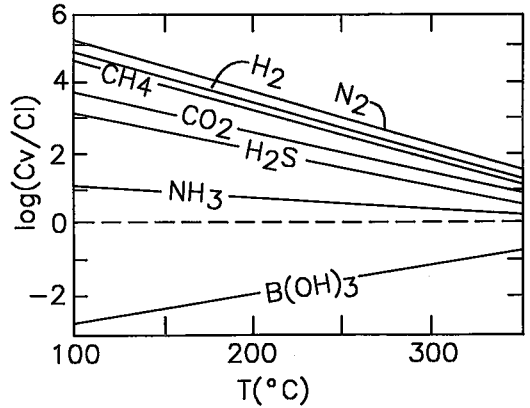


FIG. 9. Comparison of volatilities of major dissolved gases in hydrothermal systems (Giggenbach 1980) with that of boric acid (Ellis & Mahon 1977), where C_v represents the concentration in vapor and C_i represents the concentration in water. The partitioning demonstrates that boric acid is a non-volatile species. However, data are not available for very high temperatures, where partition coefficients converge.

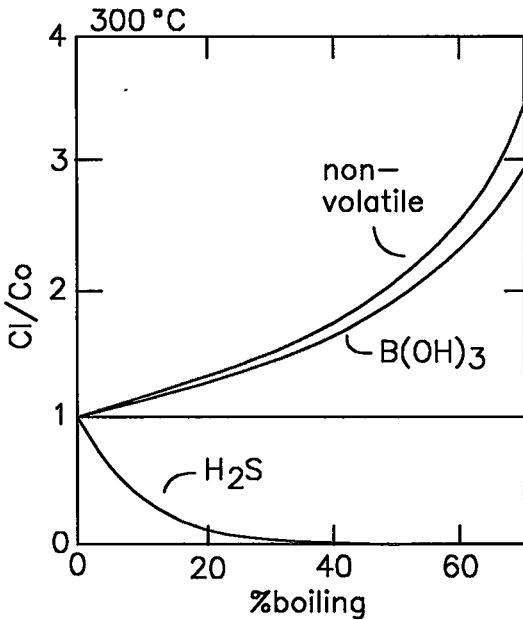


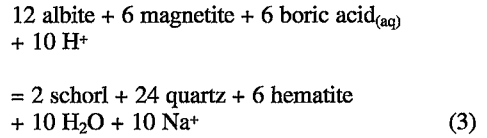
FIG. 10. Plot of an open-system (Rayleigh, partition coefficients as in Figure 9) boiling-distillation model that demonstrates segregation of the volatile species H_2S , which becomes strongly depleted in concentration within the residual fluid (C_i) relative to its initial concentration (C_o). Conversely, $B(OH)_3$ is progressively enriched in the residual fluid with increased boiling.

substance (Pichavant 1987, London *et al.* 1988). On the other hand, boric acid $B(OH)_3$ is the dominant B species in the hydrothermal regime, on the basis of studies of active geothermal systems, seafloor systems, fumaroles and volcanic emanations (e.g., Shuvalov 1974, Chiodini *et al.* 1988, Palmer 1991b, Shaw & Sturchio 1992), and on high-temperature experimental determinations and theoretical considerations (Mesmer *et al.* 1972). A number of minor polyborates may also exist (Mesmer *et al.* 1972). Boric acid has a wide range of stability and converts to borate only under conditions of very high alkalinity (Fig. 8). $B(OH)_3$ remains as the dominant species across a pH range (Chiodini *et al.* 1988, Shaw & Sturchio 1992) that encompasses all of the mineralogical zones within porphyry-alteration haloes, including potassic, phyllic, and argillic (Fig. 8). Compared to the dominant neutral and gaseous species dissolved within hydrothermal systems, boric acid is a relatively non-volatile component (Ellis & Mahon 1977) (Fig. 9), that concentrates in the residual hydrothermal fluid in boiling hydrothermal systems. Boiling consequently provides an effective mechanism for increasing B contents in hydrothermal fluids associated with porphyry systems (Fig. 10). Thus for many reasons, boric acid is an ideal choice for balancing chemical reactions involving tourmaline, and for use as a principal component on activity-activity diagrams.

Petrographic observations in the tourmaline zone of the Coxheath deposit demonstrate a close paragenetic link between tourmaline and albite: tourmaline may be directly intergrown with albite, or occur in veinlets with an albite halo. Tourmaline and albite are the two dominant Na-bearing minerals in the deposit, making up the

mineral assemblage that defines sodic alteration. To investigate the chemical changes that occurred, and those that may have controlled the precipitation of tourmaline and albite, chemical reactions were written for the system H–B–O–Na–Al–Si–Fe under quartz saturation, with hydrogen activity defined by the magnetite–hematite buffer, at T and P encompassing mineralization in porphyry systems. For simplicity, only schorl was considered, and, as a starting point for balancing the equations, Al was treated as an immobile element. The above assumptions were made because of the following observations: (1) quartz is ubiquitous throughout the Coxheath deposit in veinlets and as a replacement mineral, (2) although tourmaline at Coxheath contains approximately equal proportions of Fe and Mg, compositions of tourmaline from other porphyry systems are mainly schorl-rich, and (3) magnetite and hematite occur together in the core of the Coxheath deposit and in the tourmaline zone.

The following reaction models the coexistence of tourmaline and albite:



This reaction requires the presence of important quantities of iron oxides, which are, along with other iron-bearing minerals such as pyrite, irregularly dispersed in the Coxheath deposit, whereas tourmaline and albite are closely intergrown at a microscopic scale. Both magnetite and hematite occur in the potassic assemblage that was overprinted by the tourmaline stockwork, suggesting that the magnetite–hematite buffer provided a useful means of balancing iron and fixing the hydrogen fugacity in the system. Also, this buffer is

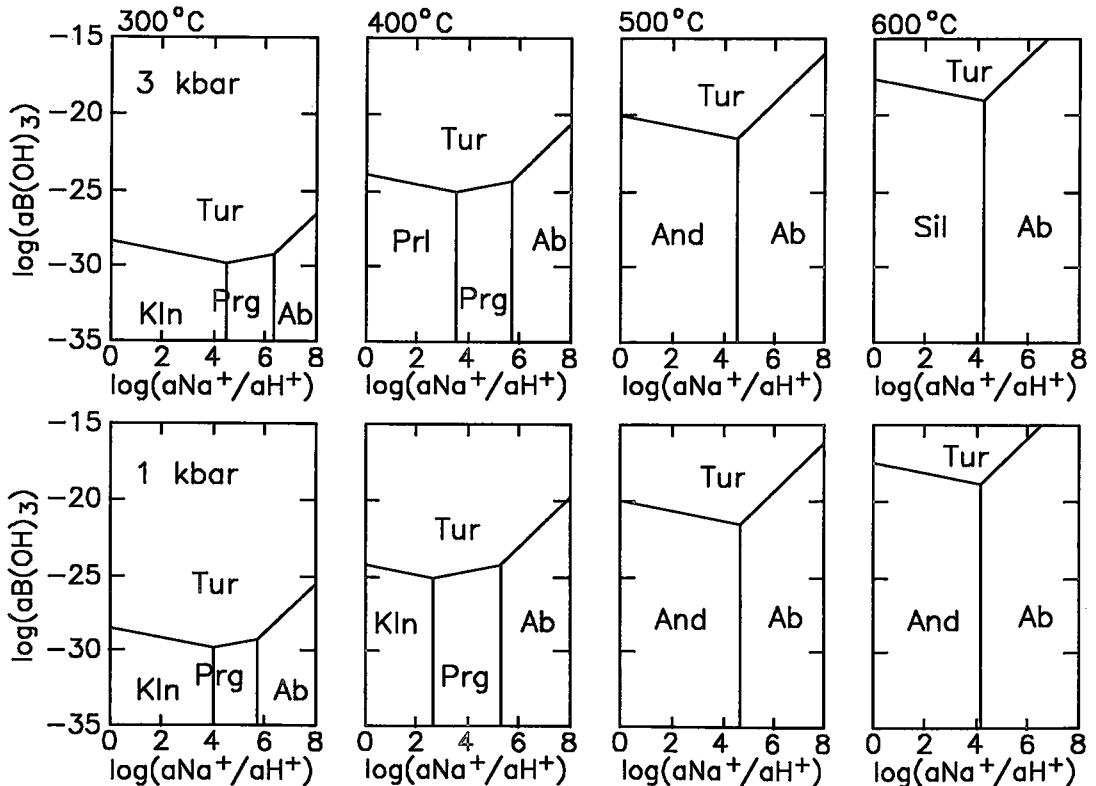


FIG. 11. Activity diagrams generated at 1 and 3 kbar pressure and from 300° to 600°C for tourmaline (Tur), albite (Ab), paragonite (Prg), andalusite (And), sillimanite (Sil), pyrophyllite (Prl), and kaolinite (Kln), in presence of quartz – magnetite – hematite – water. Diagrams indicate an expanding field of stability of tourmaline upon cooling, and show that the Na^+/H^+ ion ratio only significantly affects tourmaline stability relative to albite. Thermodynamic data are taken Kuyunko *et al.* (1984) for tourmaline, from Shock *et al.* (1989) for boric acid, and from Helgeson *et al.* (1978) for other silicates. Adjustments to equilibrium constants to high temperatures were made using the Maier & Kelley (1932) power-series equation for heat capacities; the effects of pressure on equilibrium constants were estimated by determining volumetric changes assuming incompressible reactants.

typically used when calculating mineral equilibria in porphyry-Cu systems (e.g., Beane 1982). Inspection of equation (3) reveals that iron obtained from the breakdown of magnetite is distributed between hematite and tourmaline, which is consistent with the presence of ferric iron in the Coxheath tourmaline. Also, relative to albite, tourmaline becomes stable with decreasing pH, which is consistent with the experimental work of Morgan & London (1989). Figure 11 is an activity–activity diagram displaying mineral equilibria for temperatures ranging from 300° to 600°C and pressures of 1–3 kilobars. Mineral equilibria were calculated using data from Kuyunko *et al.* (1984) for tourmaline, Shock *et al.* (1989) for boric acid, and Helgeson *et al.* (1978) for other silicates. Adjustments to equilibrium constants for high temperatures were calculated using a power-series equation for heat capacities (Maier & Kelley 1932) and assuming incompressible reactants in an evaluation of the effects of pressure. Under all conditions, tourmaline is stable at a high activity of boric acid. However, the stability field for tourmaline is strongly affected by temperature, and expands greatly upon cooling. The Na^+/H^+ value also affects relative mineral stabilities, but the steeper slope of the reaction boundary between tourmaline and albite compared to the slopes for reactions involving mica, clay, and alkali-free aluminosilicates, indicates that the ratio Na^+/H^+ is relatively less important for the latter equilibria.

DISCUSSION AND CONCLUSIONS

Although most porphyry deposits occur in Mesozoic and Cenozoic volcano–plutonic arcs, an increasing number are being recognized in Precambrian terranes. The Coxheath deposit is a good example of a Cu–Mo–Au mineralized porphyry from the Proterozoic, which displays alteration and zoning patterns typical of younger, well-characterized deposits. The presence of clay alteration at Coxheath shows that argillic alteration linked to porphyry systems may also occur in Precambrian examples. Furthermore, the Coxheath deposit contains a number of features that distinguish it as a Au-bearing porphyry (Sillitoe 1993), including (1) disseminated mineralization that yields assays near or above 4 ppm Au, as well as a positive correlation between Au and Cu (data from unpublished assessment files in provincial archives), (2) the presence of magnetite as an important hydrothermal mineral in the Au zone, (3) occurrence of both calcic and sodic alteration subtypes within the potassic zone, and (4) the predominance of propylitic alteration over phyllic alteration in the zone immediately next to the potassic core. Consequently, the Coxheath deposit, together with a number of other porphyry deposits (Hollister *et al.* 1974) and epithermal deposits such as Hope Brook in Newfoundland (Stewart 1992, Dubé *et al.* 1996), help define the Avalon Zone of the Appalachian orogen as a potentially significant

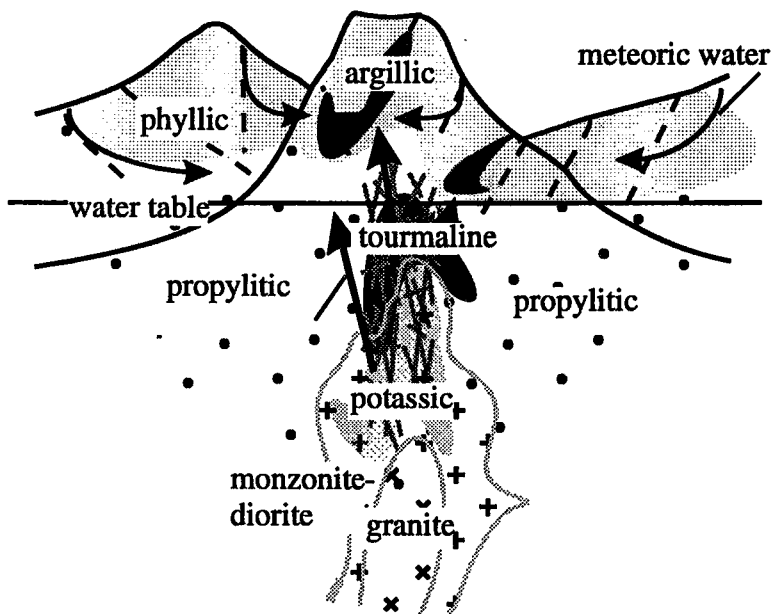


FIG. 12. Generalized diagram illustrating volcano-plutonic setting for the Coxheath Cu–Mo–Au deposit and the distribution of principal zones of alteration (see text for detailed description).

metallogenic province for porphyry-epithermal systems.

Tourmaline is an accessory mineral associated with potassic and phyllic alteration zones and hydrothermal breccias in numerous porphyry-Cu deposits (*e.g.*, Sillitoe & Sawkins 1971, Camus 1975, Gustafson & Hunt 1975, Gustafson & Quiroga 1995), and in some cases is linked directly to sodic-calcic alteration subtypes (Carten 1986, Dilles & Einaudi 1992). Mineral zonation and paragenesis at Coxheath, as at other deposits, provide important information regarding hydrothermal processes in porphyry systems (Fig. 12). Typically, potassic alteration in the core of porphyry systems is directly linked to late-magmatic hydrothermal fluids in crystallizing plutons (*e.g.*, Lowell & Guilbert 1970, Beane & Titley 1981, Sillitoe 1993, Hedenquist & Lowenstern 1994). This is likely true at Coxheath as well, because of the direct link between the potassic zone and the intrusive rocks. Furthermore, a link to magmatic-hydrothermal processes can also be inferred for the sodic alteration because of the mineralogical association; experimental work by Pichavant (1981, 1987) has shown that with the addition of B to granitic melts, the aqueous vapor phase coexisting with the melts becomes enriched in Na relative to K, and that B also is partitioned into the vapor phase relative to the melt (as NaBO_2 , among others). Thus the tendency for paired exsolution of B and Na from a crystallizing magma is possibly indicated by the close association of tourmaline and albite, together as an alteration assemblage at Coxheath. Strong temperature-gradients are also expected with magmatic-hydrothermal processes, and at Coxheath, decreasing temperature during the course of mineraliza-

tion is indicated by textures recorded in sulfides, oxides, and silicates: the development of a rim of bornite on chalcopyrite, and of hematite on magnetite (Fig. 13), as well as hydrothermal alteration of K-feldspar to muscovite, are all features that can be indicative of decreasing temperature. Furthermore, it has been shown in the activity diagrams that the stability field of tourmaline relative to those of albite, paragonite, and clay minerals increases significantly during cooling. However, tourmaline occupies a restricted area in the Coxheath system; it separates the outer pyrite-enriched zone, characterized by acidic alteration assemblages, from the pyrite-depleted core, characterized by more strongly alkaline alteration assemblages. Investigations at a number of deposits have shown that boiling is an important hydrothermal process in the formation of porphyry deposits, and that the escape and condensation of acid volatile species contribute to the formation of argillic alteration adjacent to or above the potassic core, effectively segregating mineralogical domains (*e.g.*, Hedenquist & Lowenstern 1994). Tourmaline precipitation can be placed in a context of boiling by considering the behavior of boric acid in the hydrothermal environment. Fluid-mineral equilibria suggest that tourmaline precipitation is strongly influenced by the activity of boric acid $\text{B}(\text{OH})_3$, which is concentrated in the residual hydrothermal fluid during boiling. Thus for porphyry systems, B may be concentrated in two stages, first as an incompatible element in granitic melts, and subsequently as a nonvolatile component of boiling-water-dominated hydrothermal systems. Tourmaline at the Coxheath deposit is found adjacent to the core zone, where tourmaline precipitation may have been induced by boiling. If this was

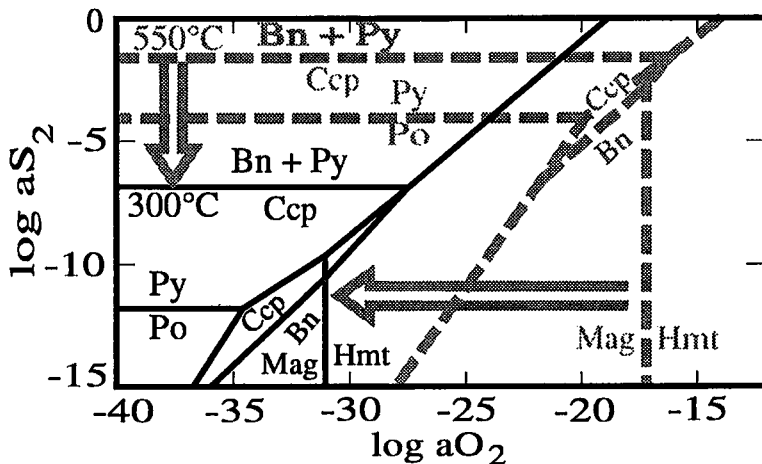


FIG. 13. Activity diagram illustrating stability fields of the principal opaque mineral phases from the Coxheath deposit, at relatively high (550°C, dashed lines) and low (300°C) temperatures. Note significant expansion of the stability fields of bornite + pyrite and hematite relative to those of chalcopyrite and magnetite upon cooling (arrows), which may promote the formation of bornite and hematite rims in Coxheath samples (Fig. 4). Modified from Beane & Titley (1981).

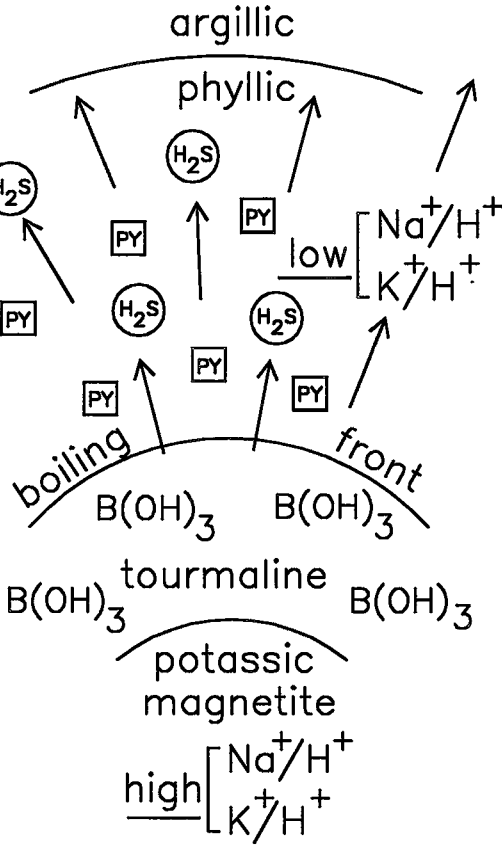


FIG. 14. Schematic model depicting context for tourmalinization within a boiling porphyry-related hydrothermal system. Segregation of acidic and alkaline alteration zones based on loss of acidic volatiles (e.g., H_2S) from the core of the system results in increased boric acid content within the residual fluid, thus promoting tourmalinization along the boiling front.

the case, then the position of the tourmaline zone delineates the boiling interface within the deposit (Fig. 14). This is consistent with results of a number of studies done on fluid inclusions in tourmaline (Skewes 1992) and within intergrown quartz (Sillitoe & Sawkins 1971, Carlson & Sawkins 1980) from other porphyry Cu deposits, which indicate that tourmaline was precipitated during boiling from hypersaline fluids.

Tourmaline compositions at Coxheath may also provide information on the mineralizing environment; relatively low aluminum and high iron contents suggest that ferric iron is an important constituent. Compositional trends characterize the tourmaline as povondraite. The presence of ferric iron in tourmaline at Coxheath and in similar deposits may be interpreted to indicate relatively oxidizing environments for porphyry-copper mineralization compared to tourmalines from most

granite-related Sn \pm W deposits, which typically contain more aluminum and little or no ferric iron (e.g., London & Manning 1995, Slack 1996). This is substantiated by the common presence of magnetite and hematite in porphyry-copper deposits, and the scarcity of these minerals in most Sn \pm W deposits.

The presence of tourmaline may also be an indicator of material provenance. Typically, in volcanic arcs, B isotope studies have shown that B is principally derived from subducted sediments (e.g., Palmer 1991a). Consequently, the presence of tourmaline in some porphyry Cu deposits, such as Coxheath, may be interpreted to indicate the incorporation into the hydrothermal system of material from a subducted slab, subsequent to plutonic-volcanic recycling. However, for deposits that are surrounded by argillaceous sedimentary rocks, local derivation of B from the host rocks seems more likely.

ACKNOWLEDGEMENTS

Support for this project was received from the Canada – Nova Scotia Cooperation Agreement on Mineral Development 1992–95, and from the Geological Survey of Canada. Guidance during the electron-microprobe sessions and data processing was given by G. Pringle and J.A.R. Stirling; XRD analysis of clay minerals was performed by A. Chagnon. Field assistance was provided by N. Fagnan and D. Pankewich. We are grateful to B.E. Taylor, W.D. Sinclair, and K. Schrijver for comments on a preliminary draft of this paper. Extensive reviews, and close attention to detail from journal referees J.F. Slack and J.T. O'Connor, resulted in a much improved manuscript.

REFERENCES

- AHLFELD, F. (1945): The Chicote tungsten deposit, Bolivia. *Econ. Geol.* **40**, 394–407.
- BARR, S.M. (1993): Geochemistry and tectonic setting of late Precambrian volcanic and plutonic rocks in southeastern Cape Breton Island, Nova Scotia. *Can. J. Earth Sci.* **30**, 1147–1154.
- _____, MACDONALD, A.S. & WHITE, C.E. (1988): The Fourchu Group and associated granitoid rocks, Coxheath Hills, Eastbay Hills, and southwestern Stirling and Coastal Belts, southeastern Cape Breton Island, Nova Scotia. *Geol. Surv. Can., Open-File Rep.* **1759**.
- BEANE, R.E. (1982): Hydrothermal alteration in silicate rocks, southwestern North America. In *Advances in Geology of the Porphyry Copper Deposits, Southwestern North America* (S.R. Titley, ed.). The University of Arizona Press, Tucson, Arizona (117–138).
- _____ & TITLEY, S.R. (1981): Porphyry copper deposits. II. Hydrothermal alteration and mineralization. *Econ. Geol., Seventy-Fifth Anniv. Vol.*, 235–269.

- BEATON, W.W. & SUGDEN, F.J. (1930): Coxheath copper mine, Cape Breton, N.S. *Can. Inst. Mining Metall. Bull.* **23**, 834-842.
- BEBOUT, G.E., RYAN, J.G. & LEEMAN, W.P. (1993): B-Be systematics in subduction-related metamorphic rocks: characterization of the subducted component. *Geochim. Cosmochim. Acta* **57**, 2227-2237.
- BEVIER, M.-L., BARR, S.M., WHITE, C.E. & MACDONALD, A.S. (1993): U-Pb geochronologic constraints on the volcanic evolution of the Mira (Avalon) terrane, southeastern Cape Breton Island, Nova Scotia. *Can. J. Earth Sci.* **30**, 1-10.
- BURT, D.M. (1989): Vector representation of tourmaline compositions. *Am. Mineral.* **74**, 826-839.
- CAMUS, F. (1975): Geology of the El Teniente orebody with emphasis on wall-rock alteration. *Econ. Geol.* **70**, 1341-1372.
- CARLSON, S.R. & SAWKINS, F.J. (1980): Mineralogic and fluid inclusion studies of the Turmalina Cu-Mo-bearing breccia pipe, northern Peru. *Econ. Geol.* **75**, 1233-1238.
- CARTEN, R.B. (1986): Sodium-calcium metasomatism: chemical, temporal, and spatial relationships at the Yerrington, Nevada, porphyry copper deposit. *Econ. Geol.* **81**, 1495-1519.
- CHATTERJEE, A.K. & OLDALE, H.R. (1980): Porphyry copper-molybdenum \pm gold mineralization at Coxheath. *Geol. Assoc. Can. - Mineral. Assoc. Can., Fieldtrip Guidebook* **6**, 3-10.
- CHIODINI, G., COMODI, P. & GIAQUINTO, S. (1988): Ammonia and boric acid in steam and water, experimental data from geothermal wells in the Phlegrean fields, Naples, Italy. *Geotherm.* **17**, 711-718.
- CLARKE, D.B., REARDON, N.C., CHATTERJEE, A.K. & GREGOIRE, D.C. (1989): Tourmaline composition as a guide to mineral exploration: a reconnaissance study from Nova Scotia using discriminant function analysis. *Econ. Geol.* **84**, 1921-1935.
- DILLES, J.H. & EINAUDI, M.T. (1992): Wall-rock alteration and hydrothermal flow paths about the Ann-Mason porphyry copper deposit, Nevada - a 6-km vertical reconstruction. *Econ. Geol.* **87**, 1963-2001.
- DOSTAL, J. & McCUTCHEON, S.R. (1990): Geochemistry of Late Proterozoic basaltic rocks from southeastern New Brunswick, Canada. *Precambrian Res.* **47**, 83-98.
- DUBÉ, B., LAUZIÈRE, K., ROBERT, F. & POULSEN, K.H. (1996): The Hope Brook gold deposit: example of an acid sulphate intrusion-related gold deposit in Newfoundland. *Geol. Surv. Can., Mineral. Colloquium* (abstr.).
- ELLIS, A.J. & MAHON, W.A. (1977): *Chemistry of Geothermal Systems*. Academic Press, London, U.K.
- ETHIER, V.G. & CAMPBELL, F.A. (1977): Tourmaline concentrations in Proterozoic sediments of the southern Cordillera of Canada and their economic significance. *Can. J. Earth Sci.* **14**, 2348-2363.
- FOIT, F.F., JR., FUCHS, Y. & MYERS, P.E. (1989): Chemistry of alkali-deficient schorls from two tourmaline-dumortierite deposits. *Am. Mineral.* **74**, 1317-1324.
- FORSYTHE, D.L. & HIGGINS, N.C. (1990): Mount Carbine tungsten deposit. In *Geology of the Mineral Deposits of Australia and Papua New Guinea* (F.E. Hughes, ed.). Australasian Institute of Mining and Metallurgy, Melbourne, Australia (1557-1560).
- FUCHS, Y. & MAURY, R. (1995): Borosilicate alteration associated with U-Mo-Zn and Ag-Au-Zn deposits in volcanic rocks. *Mineral. Deposita* **30**, 449-459.
- FUH, TSU-MIN (1965): A hydrothermal breakdown of tourmaline at high temperatures. *Acta Geol. Taiwan* **11**, 21-29.
- GIESKES, J.M. (1974): *The Sea*. Wiley-Interscience, New York, N.Y.
- GIGGENBACH, W.F. (1980): Geothermal gas equilibria. *Geochim. Cosmochim. Acta* **44**, 2021-2032.
- GOLDSCHMIDT, V.M. & PETERS, C. (1932): The chemistry of boron. II. *Nach. Ges. Wiss., Göttingen, Math. Phys. Kl.* **31**.
- GRICE, J.D., ERCIT, T.S. & HAWTHORNE, F.C. (1993): Povondraite, a redefinition of the tourmaline ferridravite. *Am. Mineral.* **78**, 433-436.
- GUSTAFSON, L.B. & HUNT, J.P. (1975): The porphyry copper deposit at El Salvador, Chile. *Econ. Geol.* **70**, 857-912.
- _____ & QUIROGA, J.G. (1995): Patterns of mineralization and alteration below the porphyry copper orebody at El Salvador, Chile. *Econ. Geol.* **90**, 2-16.
- HARDER, H. (1959): Beitrag zur Geochemie des Bors. II. Bor in Sedimenten. *Nachr.* **6**, 123-183.
- HAWTHORNE, F.C. (1996): Structural mechanisms for light-element variations in tourmaline. *Can. Mineral.* **34**, 123-132.
- HEDENQUIST, J.W. & LOWENSTERN, J.B. (1994): The role of magmas in the formation of hydrothermal ore deposits. *Nature* **370**, 519-527.
- HELGESON, H.C., DELANY, J.M., NESBITT, H.W. & BIRD, D.K. (1978): Summary and critique of the thermodynamic properties of rock-forming minerals. *Am. J. Sci.* **278-A**, 1-229.
- HENRY, D.J. & DUTROW, B.L. (1992): Tourmaline in a low grade clastic metasedimentary rock: an example of the petrogenetic potential of tourmaline. *Contrib. Mineral. Petrol.* **112**, 203-218.
- _____ & GUIDOTTI, C.V. (1985): Tourmaline as a petrogenetic indicator mineral: an example from the staurolite-grade metapelites of NW Maine. *Am. Mineral.* **70**, 1-15.

- HOLLISTER, V.F., POTTER, R.R. & BARKER, A.L. (1974): Porphyry-type deposits of the Appalachian orogen. *Econ. Geol.* **69**, 618-630.
- HSU, KE-CHIN (1943): Tungsten deposits in southern Kiangsi, China. *Econ. Geol.* **38**, 431-474.
- ISHIKAWA, T. & NAKAMURA, E. (1994): Origin of the slab component in arc lavas from across-arc variation of B and Pb isotopes. *Nature* **370**, 205-208.
- JOLIFF, B.L., PAPIKE, J.J. & SHEARER, C.K. (1986): Tourmaline as recorder of pegmatite evolution: Bob Ingersoll pegmatite, Black Hills, South Dakota. *Am. Mineral.* **71**, 472-500.
- KEPPIE, J.D., DALLMEYER, R.D. & MURPHY, J.B. (1990): Tectonic implication of $^{40}\text{Ar}/^{39}\text{Ar}$ hornblende ages from Late Proterozoic – Cambrian plutons in the Avalon composite terrane, Nova Scotia, Canada. *Geol. Soc. Am. Bull.* **102**, 516-528.
- KING, R.W. (1990): *Tourmaline from Mesothermal Gold Deposits of the Superior Province, Canada: Textural, Chemical and Isotopic Relationships*. Ph.D. thesis, Univ. of Saskatchewan, Saskatoon, Saskatchewan.
- _____ & KERRICH, R.W. (1986): Tourmaline in Archean lode gold deposits. 1. Geochemical characteristics. *Geol. Soc. Am., Abstr. Programs*, **18**, 657.
- KOVAL, P.V., ZORINA, L.D., KITAJEV, N.A., SPIRIDONOV, A.M. & ARIUNBLEG, S. (1991): The use of tourmaline in geochemical prospecting for gold and copper mineralization. *J. Geochem. Explor.* **40**, 349-360.
- KRYNINE, P.D. (1946): The tourmaline group in sediments. *J. Geol.* **54**, 65-87.
- KUYUNKO, N.S., SEMONOV, Y.V., GOREVICH, V.M., KUZ'MIN, V.I., TOPOR, N.D. & GORBUNOV, V.Y. (1984): Experimental determination of the thermodynamic properties of tourmaline–dravite. *Geochem. Int.* **22**, 109-116.
- LANDERGREN, S. (1945): Contribution to the geochemistry of boron. II. *Arkiv. Kemi Mineral. Geol.* **19A**, 26.
- LEEMAN, W.P., CARR, M.J. & MORRIS, J.D. (1994): Boron geochemistry of the Central American volcanic arc: constraints on the genesis of subduction-related magmas. *Geochim. Cosmochim. Acta* **58**, 149-168.
- LONDON, D., HERVIG, R.L. & MORGAN, G.B., VI (1988): Melt-vapor solubilities and elemental partitioning in peraluminous granite–pegmatite systems: experimental results with Macusani glass at 200 MPa. *Contrib. Mineral. Petrol.* **99**, 360-373.
- _____ & MANNING, D.A.C. (1995): Chemical variation and significance of tourmaline from southwest England. *Econ. Geol.* **90**, 495-519.
- LOWELL, J.D. & GUILBERT, J.M. (1970): Lateral and vertical alteration – mineralization zoning in porphyry ore deposits. *Econ. Geol.* **65**, 373-408.
- LUBIS, H., PRIHATMOKO, S. & JAMES, L.P. (1994): Bulagidun prospect: a copper, gold, and tourmaline bearing porphyry and breccia system in northern Sulawesi, Indonesia. *J. Geochem. Explor.* **50**, 257-278.
- LYNCH, J.V.G. (1989): Hydrothermal alteration, veining, and fluid inclusion characteristics of the Kalzas wolframite deposit, Yukon. *Can. J. Earth Sci.* **26**, 2106-2115.
- MAIER, C.G. & KELLEY, K.K. (1932): An equation for the high temperature heat content data. *J. Am. Chem. Soc.* **54**, 3243-3246.
- MAO, JINGWEN (1995): Tourmalinite from northern Guangxi, China. *Mineral. Deposita* **30**, 235-245.
- MELDRUM, S.J., AQUINO, R.S., GONZALES, R.I., BURKE, R.J., SUYADI, A., IRIANTO, B. & CLARKE, D.S. (1994): The Batu Hijau porphyry copper–gold deposit, Sumbawa Island, Indonesia. *J. Geochem. Explor.* **50**, 203-220.
- MESMER, R.E., BAES, C.F. & SWEETON, F.H. (1972): Acidity measurements at elevated temperatures. VI. Boric acid equilibria. *Inorg. Chem.* **11**, 537-543.
- MORGAN, G.B., VI & LONDON, D. (1989): Experimental reactions of amphibolite with boron-bearing aqueous fluids at 200 MPa: implications for tourmaline stability and partial melting in mafic rocks. *Contrib. Mineral. Petrol.* **102**, 281-297.
- OLDALE, H.R. (1967): A centennial of mining exploration and development – Coxheath Hills, Cape Breton. *Can. Inst. Mining Metall. Bull.* **60**, 1411-1419.
- PALMER, M.R. (1991a): Boron isotope systematics of Halmahera arc (Indonesia) lavas: evidence for involvement of the subducted slab. *Geology* **19**, 215-217.
- _____ (1991b): Boron isotope systematics of hydrothermal fluids and tourmalines: a synthesis. *Isotope Geosci.* **14**, 111-121.
- _____ & SLACK, J.F. (1989): Boron isotopic composition of tourmaline from massive sulfide deposits and tourmalinites. *Contrib. Mineral. Petrol.* **103**, 434-451.
- PICHAVANT, M. (1981): An experimental study of the effect of boron on a water-saturated haplogranite at 1 kbar pressure: geological applications. *Contrib. Mineral. Petrol.* **76**, 430-439.
- _____ (1987): Effects of B and H₂O on liquidus phase relations in the haplogranite system at 1 kbar. *Am. Mineral.* **72**, 1056-1070.
- POVONDRA, P. & NOVÁK, M. (1986): Tourmalines in metamorphosed carbonate rocks from western Moravia, Czechoslovakia. *Neues Jahrb. Mineral., Monatsh.*, 273-282.
- ROBBINS, C.R. & YODER, H.S., JR. (1962): Stability relations of dravite, a tourmaline. *Carnegie Inst. Wash., Year Book* **61**, 106-107.

- ROBERT, F. & BROWN, A.C. (1986): Archean gold-bearing quartz veins at the Sigma mine, Abitibi greenstone belt, Quebec. II. Vein paragenesis and hydrothermal alteration. *Econ. Geol.* **81**, 593-616.
- SHAW, D.M. & STURCHIO, N.C. (1992): Boron–lithium relationships in rhyolites and associated thermal waters of young silicic calderas, with comments on incompatible element behavior. *Geochim. Cosmochim. Acta* **56**, 3723-3731.
- SHELNUTT, J.P. & NOBLE, D.C. (1985): Premineralization radial dikes of tourmalinized fluidization breccia, Julcani district, Peru. *Econ. Geol.* **80**, 1622-1632.
- SHOCK, E.L., HELGESON, H.C. & SYRJENSKY, D.A. (1989): Calculation of the thermodynamic and transportation properties of aqueous species at high pressures and temperatures: standard partial molal properties of inorganic neutral species. *Geochim. Cosmochim. Acta* **53**, 2157-2183.
- SHUVALOV, R.A. (1974): Distribution of boric acid between water and vapor during separation of the vapor–water mixture of Puzhetka deposits. In *Hydrothermal Mineral-Forming Solutions in the Areas of Active Volcanism* (S.I. Naboko, ed.). Oxonian Press, Calcutta, India (155-159).
- SILLITOE, R.H. (1973): Geology of the Los Pelambres porphyry copper deposit, Chile. *Econ. Geol.* **68**, 1-10.
- _____ (1993): Gold-rich porphyry copper deposits: geological model and exploration implications. In *Mineral Deposit Modeling* (R.V. Kirkham, W.D. Sinclair, R.I. Thorpe & J.M. Duke, eds.). *Geol. Assoc. Can., Spec. Pap.* **40**, 465-478.
- _____ & SAWKINS, F.J. (1971): Geologic, mineralogic and fluid inclusion studies relating to the origin of copper-bearing tourmaline breccia pipes, Chile. *Econ. Geol.* **66**, 1028-1041.
- SINCLAIR, W.D. & RICHARDSON, J.M. (1992): Quartz–tourmaline orbicules in the Seagull batholith, Yukon Territory. *Can. Mineral.* **30**, 923-935.
- SKEWES, M.A. (1992): *Miocene and Pliocene Copper-Rich Breccias from the Andes of Central Chile (32°–34°S)*. Ph.D. thesis, Univ. of Colorado, Boulder, Colorado.
- SLACK, J.F. (1982): Tourmaline in Appalachian–Caledonian massive sulphide deposits and its exploration significance. *Inst. Mining Metall. Trans.* **91(B)**, B81-B89.
- _____ (1996): Tourmaline associations with hydrothermal ore deposits. In *Boron: Mineralogy, Petrology, and Geochemistry* (E.S. Grew & A.M. Anovitz, eds.). *Rev. Mineral.* **33** (in press).
- SMITH, F.G. (1949): Transport and deposition of the non-sulphide vein minerals. IV. Tourmaline. *Econ. Geol.* **44**, 186-192.
- STEWART, P.W. (1992): *The Origin of the Hope Brook Mine, Newfoundland: a Shear Zone Hosted Acid Sulphate Gold Deposit*. Ph.D. thesis, Univ. of Western Ontario, London Ontario.
- TAYLOR, B.E. & SLACK, J.F. (1984): Tourmalines from Appalachian–Caledonian massive sulfide deposits: textural, chemical, and isotopic relationships. *Econ. Geol.* **79**, 1703-1726.
- THICKE, M.J. (1987): *The Geology of Late Hadrynian Metavolcanic and Granitoid Rocks of the Coxheath – Northern East Bay Area, Cape Breton Island, Nova Scotia*. M.Sc. thesis, Acadia Univ., Wolfville, Nova Scotia.
- VORBACH, A. (1989): Experimental examinations on the stability of synthetic tourmalines in temperatures from 250°C to 750°C and pressures to 4 kb. *Neues Jahrb. Mineral., Abh.* **161**, 69-83.
- WARNAARS, F.W., HOLMGREN D.C. & BARASSI, F.S. (1985): Porphyry copper and tourmaline breccias at Los Bronces – Rio Blanco, Chile. *Econ. Geol.* **80**, 1544-1565.
- WILLIAMS, H. (1984): Miogeoclines and suspect terranes of the Caledonian – Appalachian orogen: tectonic patterns in the North Atlantic region. *Can. J. Earth Sci.* **21**, 887-901.
- YOU, C.F., SPIVACK, A.J., GIESKES, J.M., ROSENBAUER, R. & BISCHOFF, J.L. (1995): Experimental study of boron geochemistry: implications for fluid processes in subduction zones. *Geochim. Cosmochim. Acta* **59**, 2435-2442.

Received June 6, 1996, revised manuscript accepted October 3, 1996.